

## Investigation of outer valence orbital of $\text{CF}_2\text{Cl}_2$ by a new type of electron momentum spectrometer

This article has been downloaded from IOPscience. Please scroll down to see the full text article.

2005 Chinese Phys. 14 2467

(<http://iopscience.iop.org/1009-1963/14/12/016>)

View [the table of contents for this issue](#), or go to the [journal homepage](#) for more

Download details:

IP Address: 166.111.26.181

The article was downloaded on 06/05/2011 at 07:01

Please note that [terms and conditions apply](#).

# Investigation of outer valence orbital of $\text{CF}_2\text{Cl}_2$ by a new type of electron momentum spectrometer<sup>\*</sup>

Ning Chuan-Gang(宁传刚), Ren Xue-Guang(任雪光),

Deng Jing-Kang(邓景康)<sup>†</sup>, Su Guo-Lin(苏国林),

Zhang Shu-Feng(张书锋), Huang Feng(黄峰), and Li Gui-Qin(李桂琴)

*Key Laboratory of Atomic and Molecular NanoSciences, Ministry of Education, Department of Physics,  
Tsinghua University, Beijing 100084, China*

(Received 23 February 2005; revised manuscript received 12 July 2005)

Electronic states of  $\text{CF}_2\text{Cl}_2$  (dichlorodifluoromethane, Freon 12) have been studied using a new type of electron momentum spectrometer with a very high efficiency at an impact energy of 1200 eV plus binding energy. The experimental electron momentum profiles are compared with the density functional theory (DFT) and Hartree-Fock (HF) calculations. The relationship between orbital assignments in different coordinate systems is discussed. A new method of difference analysis based on the new type of electron momentum spectrometer is used to clarify the ambiguities regarding the orbital ordering.

**Keywords:** electron momentum spectroscopy,  $\text{CF}_2\text{Cl}_2$ , orbital assignment

**PACC:** 3120B, 0781

## 1. Introduction

$\text{CF}_2\text{Cl}_2$  (dichlorodifluoromethane, Freon 12) has a variety of applications, such as refrigerant, foam-blowing agent, aerosol propellant, plasma-processing agent and additive in gaseous dielectric mixtures.<sup>[1,2]</sup> It also plays an important role in stratospheric ozone depletion.<sup>[3]</sup> Electronic states of  $\text{CF}_2\text{Cl}_2$  have been extensively studied by various experimental and theoretical methods: He I and He II photoelectron spectroscopy (PES),<sup>[4,5]</sup> x-ray PES,<sup>[6]</sup> electron momentum spectroscopy (EMS),<sup>[7]</sup> Multireference Double Configuration Interaction (MRD-CI)<sup>[8,9]</sup> and outer valence Green function (OVGF) calculation.<sup>[1]</sup> However, the orbital assignments proposed by these experimental

and theoretical methods have been controversial as shown in Table 1. EMS can provide a unique way to unambiguously assign the irreducible representations to molecular orbitals experimentally by simply comparing the experimental momentum profiles with theoretical calculations.<sup>[6,10,11]</sup>

In this work, we report a new type of electron momentum spectrometer and EMS study of  $\text{CF}_2\text{Cl}_2$  at an impact energy of 1200eV plus binding energy. Experimental momentum profiles of valence orbitals are obtained and compared with various theoretical calculations. The relationship between the orbital assignments in different coordinate systems is discussed to clarify the ambiguities regarding the orbital ordering.

<sup>\*</sup>Project supported by the National Natural Science Foundation of China (Grant Nos 19854002, 19774037 and 10274040) and the Research Fund for the Doctorate Program of Higher Education (Grant No 1999000327).

<sup>†</sup>Corresponding author. E-mail: dj-k-dmp@mail.tsinghua.edu.cn

**Table 1<sup>a</sup>.** Outer valence ionization potentials (eV) and orbital ordering of CF<sub>2</sub>Cl<sub>2</sub>.

He I/He II <sup>[4]</sup>	EMS <sup>[7]</sup>	MRD-CI <sup>[7,8]</sup>	OVGf <sup>[1]</sup>	B3LYP <sup>b)</sup>	HF <sup>b)</sup>	OVGf <sup>b)</sup>
			6-311+G (d,p)	AUG-cc-pVTZ	6-311++G (3df,3pd)	6-311++G (3df,3pd)
4b <sub>1</sub> (12.26)	4b <sub>1</sub>	4b <sub>1</sub> (13.36)	4b <sub>1</sub> (11.96)	4b <sub>1</sub> (9.23)	4b <sub>1</sub> (12.97)	4b <sub>1</sub> (12.18)
4b <sub>2</sub> (12.53)	2a <sub>2</sub>	2a <sub>2</sub> (13.92)	2a <sub>2</sub> (12.33)	2a <sub>2</sub> (9.55)	2a <sub>2</sub> (13.45)	2a <sub>2</sub> (12.59)
2a <sub>2</sub> (13.11)	4b <sub>2</sub>	4b <sub>2</sub> (14.44)	4b <sub>2</sub> (12.84)	4b <sub>2</sub> (9.99)	4b <sub>2</sub> (13.95)	4b <sub>2</sub> (13.07)
6a <sub>1</sub> (13.45)	6a <sub>1</sub>	6a <sub>1</sub> (14.72)	6a <sub>1</sub> (13.15)	6a <sub>1</sub> (10.35)	6a <sub>1</sub> (14.28)	6a <sub>1</sub> (13.39)
3b <sub>1</sub> (14.36)	3b <sub>1</sub>	3b <sub>1</sub> (15.63)	3b <sub>1</sub> (14.18)	3b <sub>1</sub> (11.29)	3b <sub>1</sub> (15.41)	3b <sub>1</sub> (14.33)
3b <sub>2</sub> (15.9)	(3b <sub>2</sub> , 1a <sub>2</sub> , 5a <sub>1</sub> ) <sup>c)</sup> {	5a <sub>1</sub> (18.20)	5a <sub>1</sub> (16.29)	3b <sub>2</sub> (12.71)	5a <sub>1</sub> (17.93)	5a <sub>1</sub> (16.39)
1a <sub>2</sub> (16.30)		3b <sub>2</sub> (19.12)	3b <sub>2</sub> (16.41)	5a <sub>1</sub> (12.99)	3b <sub>2</sub> (18.72)	3b <sub>2</sub> (16.46)
5a <sub>1</sub> (16.9)		1a <sub>2</sub> (20.11)	1a <sub>2</sub> (17.21)	1a <sub>2</sub> (13.38)	1a <sub>2</sub> (19.70)	1a <sub>2</sub> (17.27)
2b <sub>2</sub> (19.3)	(2b <sub>2</sub> , 4a <sub>2</sub> ) <sup>c)</sup> {	4a <sub>1</sub> (22.25)	2b <sub>1</sub> (19.44)	2b <sub>1</sub> (15.84)	2b <sub>1</sub> (21.75)	2b <sub>1</sub> (21.75) <sup>d)</sup>
4a <sub>1</sub> (19.3)		2b <sub>1</sub> (22.27)	4a <sub>1</sub> (19.51)	4a <sub>1</sub> (15.95)	4a <sub>1</sub> (21.79)	4a <sub>1</sub> (21.79) <sup>d)</sup>
2b <sub>1</sub> (20.4)	2b <sub>1</sub>	2b <sub>2</sub> (22.85)	4b <sub>2</sub> (20.62)	2b <sub>2</sub> (16.96)	2b <sub>2</sub> (22.64)	2b <sub>2</sub> (22.64) <sup>d)</sup>
3a <sub>1</sub> (22.4)	3a <sub>1</sub>	3a <sub>1</sub> (25.98)	3a <sub>1</sub> (23.35)	3a <sub>1</sub> (19.23)	3a <sub>1</sub> (25.70)	3a <sub>1</sub> (25.70) <sup>d)</sup>

a) The irreducible representations used in Refs.[1, 7, 8] are in the *Z*-Matrix 1 coordinate system, thus they are different from those in this work in form. They are transformed into being of a unified description. The order numbers before the irreducible representation in Refs.[1, 7] include the core states. Although it does not mention which one is employed, Table II in Ref.[7] indicates that the coordinate system used is the same as that chosen in Ref.[9]. See text for details.

b) this works, implemented in GAUSSIAN 98 program.

c) Ref.[7] did not give their ordering.

d) HF-eigenvalues, OVGf calculation in GAUSSIAN 98 program did not list the corresponding optimized values.

## 2. Methods

Recently we have developed a new type of EMS spectrometer with an efficiency two orders higher than our previous one.<sup>[12]</sup> The basic principle of EMS is based on an impact ionization reaction, where the gas-phase target molecules are ionized by the high energy electron beam.<sup>[13–16]</sup> The outgoing electrons scattered and ionized are angle- and energy-selected by a toroidal energy analyser and then detected in coincidence. The experimental geometry is symmetric and non-coplanar, i.e. the two outgoing electrons are selected to have the same polar angles ( $\theta_1 = \theta_2 = 45^\circ$ , the angles included between the outgoing electron direction and the incoming electron beam direction). The azimuthal angles  $\phi$ , which are the angles included between the outgoing electron direction in the plane normal to the beam direction and the scattering plane in which  $\phi=0$ , ranging from  $-38^\circ$  to  $38^\circ$  are simultaneously measured, so the detect efficiency is much higher. The measurement typically takes only several hours, while with the previous spectrometer it takes about a month. Moreover, all binding energy spectra (BES) at different angles are collected at the

same time, so the effects of instabilities of the electron beam and gas sample intensity are greatly reduced. A profile of differential cross section versus recoil momentum for each energy-resolved state of the target molecules can be obtained from these binding energy spectra at different angles  $\phi$ . Under the binary encounter requirements of high impact energy and high momentum transfer the initial momentum  $p$  of a knocked-out electron is given by

$$p = \left\{ (2p_1 \cos\theta_1 - p_0)^2 + [2p_1 \sin\theta_1 \sin(\phi/2)]^2 \right\}^{1/2}, \quad (1)$$

where  $p_1$  and  $p_2$  ( $p_1 = p_2$ ) are the momenta respectively for the two outgoing electrons and  $p_0$  is the momentum of an incident electron.

In the planar wave impulse approximation (PWIA), the EMS binary (e, 2e) differential cross section for randomly oriented gas-phase molecules is given by<sup>[15]</sup>

$$\sigma_{\text{EMS}} \propto S_j^f \int d\Omega |\psi_j(p)|^2, \quad (2)$$

where  $\psi_j(p)$  is the independent-particle momentum space wavefunction for the  $j$ th electron that comes from ionization.  $S_j^f$  is called spectroscopic factor or

pole strength. The integral in Eq.(2) is known as the spherically averaged one-electron momentum distribution. Therefore EMS has the ability to image the electron density distributions in individual orbitals selected according to their binding energies.

In EMS, the individual orbitals are selected by binding (or ionization) energies. With the multichannel energy dispersive spectrometer used in the present work, binding energy spectra are collected at various azimuthal angles  $\phi$ . Distributions as a function of angle  $\phi$  are obtained by use of deconvolution of these BES using Gaussian functions located at each ionization energy. The widths of the Gaussian functions can be determined in consideration of published PES vibronic manifolds and the instrumental energy resolution. For each ionization process, set of areas of fitted peaks are plotted as a function of momentum calculated from  $\phi$  using Eq.(1). To compare the experimental momentum distributions with the relative cross sections calculated as a function of momentum using Eq.(2) above, the effects of the finite spectrometer acceptance angles  $\theta$  and  $\phi$  ( $\Delta\theta \approx \pm 0.7^\circ$  and  $\Delta\phi \approx \pm 1.9^\circ$ ) must be included. This was achieved in the present work with the Gaussian method.<sup>[17]</sup>

The gaseous sample of  $\text{CF}_2\text{Cl}_2$  measured in this work is 99% purity, and was used directly without further purification. No impurities are observed in the binding energy spectra.

### 3. Results and discussion

$\text{CF}_2\text{Cl}_2$  has  $C_{2v}$  point group symmetry in its ground state, and its orbitals' irreducible representations are  $B_1$ ,  $B_2$ ,  $A_1$  and  $A_2$ . In some theoretical and experimental studies on  $\text{CF}_2\text{Cl}_2$ , such a coordinate system is chosen that the  $b_2$  orbitals have a nodal surface in the F-C-F plane ( $Z$ -matrix 1, see footnote of Table 1 in Ref.[9]). In principle, it is possible to employ another coordinate system in which the irreducible representation of the molecular orbitals, which have a nodal surface in the F-C-F plane, becomes  $b_1$  ( $Z$ -matrix 2). It should be noted that the  $b_1$  and  $b_2$  orbitals in the former coordinate system correspond to the  $b_2$  and  $b_1$  orbitals in the latter one, respectively. The two coordinate systems are given in the appendix, and the coordinate system used in this work is  $Z$ -matrix 2. For the convenience of description, the assignments of orbitals throughout this paper are the same as those obtained finally in this paper except some cases with special statements.

The outer valence BES of  $\text{CF}_2\text{Cl}_2$  is measured in

a range from 10 to 33 eV. Figure 1 shows the angle-resolved binding spectra map as well as the summed one over all  $\phi$  angles. Since EMS spectrometer cannot identify each orbital from BES, only nine Gaussian peaks are fitted to BES for the 12 outer valence orbitals and two inner valence orbitals, which are shown as the dotted lines in Fig.1. The averaged ionization potentials for  $4b_1+2a_2$ ,  $4b_2+6a_1$ ,  $3b_1$ ,  $5a_1+3b_2+1a_2$ ,  $2b_1+4a_1$ ,  $2b_2$  and  $3a_1$  are determined to be 12.40, 13.28, 14.26, 16.30 19.30, 20.40 and 22.40 eV respectively, and their widths are combinations of the EMS instrumental energy resolution (FWHM=1.2 eV) with the corresponding Franck-Condon widths derived from high-resolution PES data. Some spectroscopic strength over 25 eV is contributed from inner valence orbitals and satellite lines. The solid line represents the sum of these peaks.

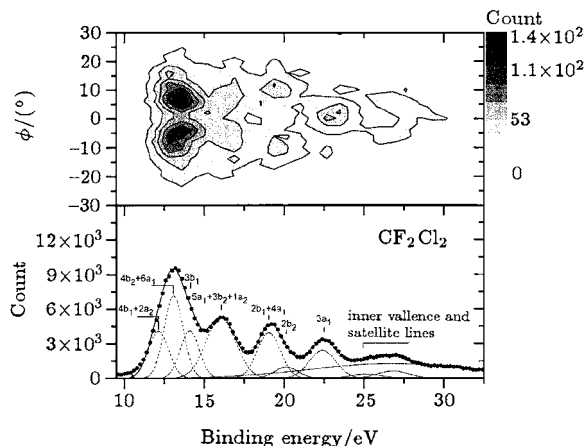


**Fig.1.** Angle-resolved binding energy map and sum of all  $\phi$  angles of  $\text{CF}_2\text{Cl}_2$ . The dashed and solid lines represent individual and summed Gaussian fits, respectively.

To obtain the experimental momentum profiles, the binding energy spectra are grouped according to different angles  $\phi$  in steps of  $1^\circ$ . The experimental momentum profiles are extracted by deconvoluting the same peak from the binding energy spectra at different  $\phi$  angles. As shown in Fig.2, the experimental momentum distributions of  $\text{CF}_2\text{Cl}_2$  are compared with various theoretical momentum profiles. Except for  $5a_1+3b_2+1a_2$ , the density functional theory (B3LYP with AUG-cc-pVTZ and 6-311++G(3df, 3pd) basis sets) and Hartree-Fock (HF with AUG-cc-pVTZ, 6-311++G(3df, 3pd) and 6-31G basis sets) calculations can well reproduce the experimental momentum distributions in general, so the PWIA is reasonable in calculations for these orbitals. This is the theoretical

foundation for the orbital assignments in this work. The fail in theoretical descriptions of  $5a_1+3b_2+1a_2$  may be due to the distorted wave effects because the fluorine lone pairs in  $1a_2$  orbital have some d-

like symmetry.<sup>[18–23]</sup> Our recent work about the  $1b_{3g}$  orbital of ethylene presents more details about this effect.<sup>[24]</sup>

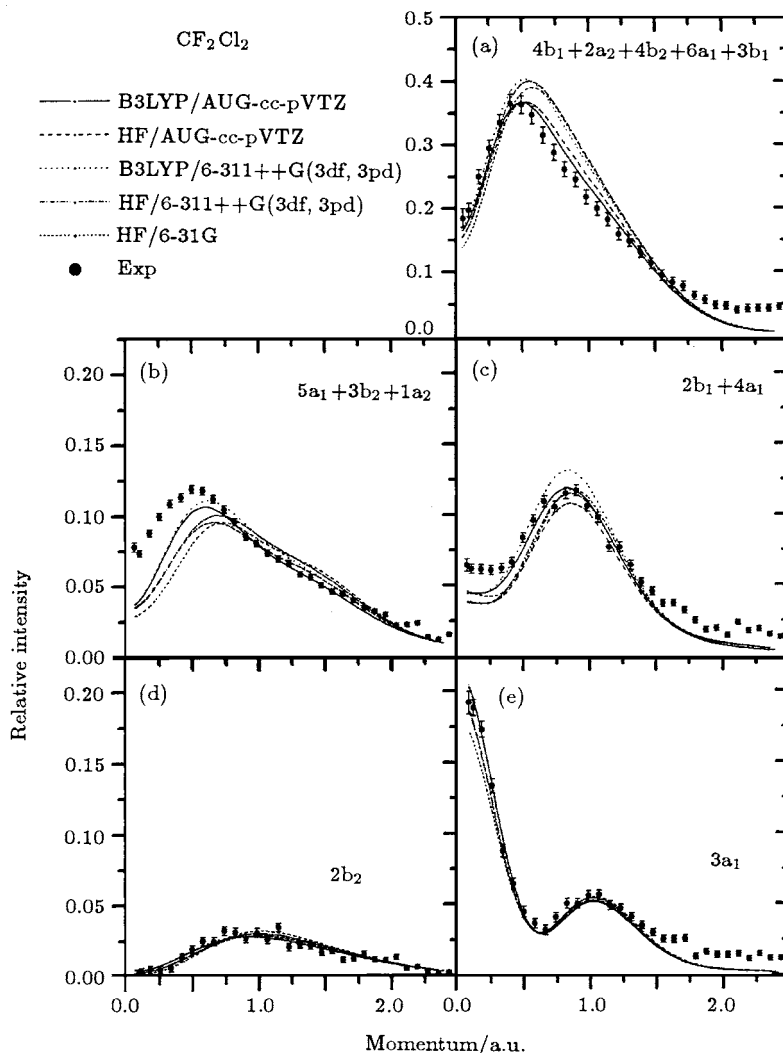


**Fig. 2.** Measured and calculated spherically averaged momentum profiles for  $4b_1+2a_2+4b_2+6a_1+3b_1$ ,  $3b_2+5a_1+1a_2$ ,  $2b_1+4a_1$ ,  $2b_2$  and  $3a_1$  orbitals of  $CF_2Cl_2$ .

High-resolution PES shows that there are five orbitals located at 12.26, 12.53, 13.11, 13.45 and 14.36 eV. As Table I shows, Ref.[5] proposed the following ordering for the five highest-occupied orbitals:

I:  $4b_1 < 4b_2 < 2a_2 < 6a_1 < 3b_1$ ,  
 while Refs.[1, 6–8] and the calculations in this work suggest

II:  $4b_1 < 2a_2 < 4b_2 < 6a_1 < 3b_1$ .

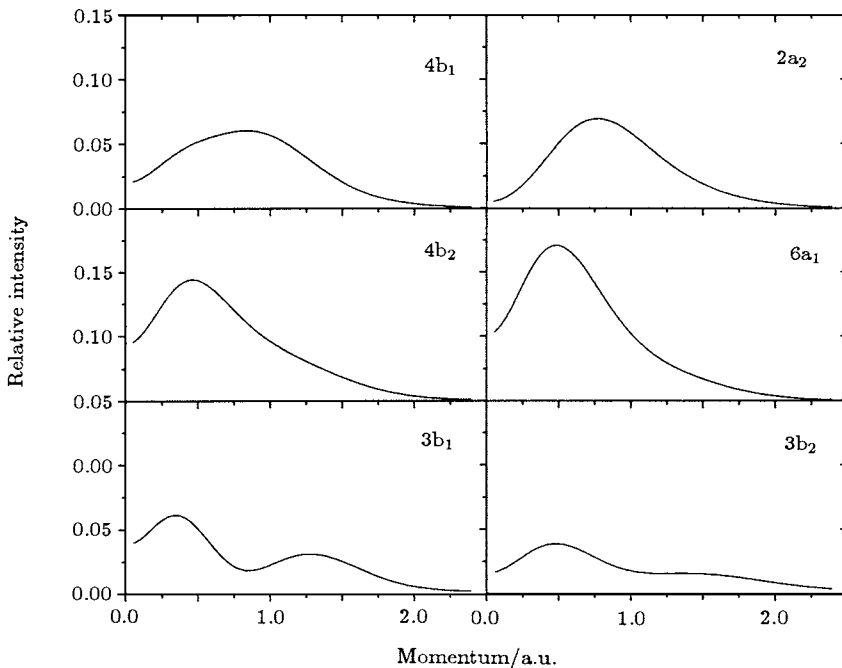


**Fig.3.** Theoretical spherically averaged momentum profiles of 4b<sub>1</sub>, 2a<sub>2</sub>, 4b<sub>2</sub>, 6a<sub>1</sub>, 3b<sub>1</sub> and 3b<sub>2</sub> orbitals of CF<sub>2</sub>Cl<sub>2</sub>, which are folded with the instrumental momentum resolution.

The theoretical momentum profiles of the five highest-occupied orbitals are highly characteristic as shown in Fig.3, so it should be easy to assign them if individual momentum profiles are observed. Unfortunately, it is impossible for the present EMS spectrometer due to the small energy-spacing between these orbitals. An alternative approach must be taken to resolve this problem. If we cut the energy region into two energy slices at 11.9–12.8eV (defined as Left) and 12.8–13.7eV (Right) in the map of Fig.1, it is expected that there is a difference between the theoretical momentum profiles in the two energy slices due to the different ordering. To elucidate this clearly, the following variables are defined:

$$I(p)_{\text{Left}} = \int_{11.9}^{12.8} \sum_i \rho_i(p) \frac{1}{\sqrt{2\pi}a_i} \exp\left(-\frac{(E - \varepsilon_i)^2}{2a_i^2}\right) dE,$$

$$I(p)_{\text{Right}} = \int_{12.8}^{13.7} \sum_i \rho_i(p) \frac{1}{\sqrt{2\pi}a_i} \exp\left(-\frac{(E - \varepsilon_i)^2}{2a_i^2}\right) dE,$$

$$\Delta I(p)_{\text{Th}} = I(p)_{\text{Right}} - I(p)_{\text{Left}}, \quad (3)$$

where  $\rho_i(p)$  is the theoretical momentum profile (incorporated with experimental momentum resolution) of the  $i$ th orbital. Since the main contributions in this energy region are from orbitals 4b<sub>1</sub>, 2a<sub>2</sub>, 4b<sub>2</sub>, 6a<sub>1</sub>, and 3b<sub>1</sub>, other orbitals' contributions are not included in calculations.  $\varepsilon_i$  is the ionization potential of the  $i$ th

orbital obtained from PES, and  $a_i = \frac{\text{FWHM}_i}{2\sqrt{\ln 4}}$  (in this case, all  $\text{FWHM}_i = 1.4$  eV).

Correspondingly, the experimental data are given by

$$\Delta_{\text{Exp}}(p) = \sum_{E=12.8}^{13.7} I_{\text{Exp}}(E, p) - \sum_{E=11.9}^{12.8} I_{\text{Exp}}(E, p), \quad (4)$$

where  $I_{\text{Exp}}(E, p)$  is the experimental intensity as shown in the map (see Fig.1), and the momentum  $p$  is related to  $\phi$  by Eq.(1). As illustrated in Fig.4, it is obvious that the ordering of II describes the experimental data better than the ordering of I, so the correct order should be 4b<sub>1</sub> < 2a<sub>2</sub> < 4b<sub>2</sub> < 6a<sub>1</sub> < 3b<sub>1</sub>. Generally, DFT with larger basis sets describes the experimental momentum distributions better than HF in a lower momentum region, so the calculation is at B3LYP/AUG-cc-pVTZ level. The discrepancy between calculations and measurements in a 0.5 a.u. <  $p$  < 1.5 a.u. momentum region may result from the small discrepancy between calculations and measure in Fig.2(a). It should be noted that the normalized factor for the experimental data in Fig.4 must be the same as those in Fig.2(a). The errors mainly come from the experimental statistic errors, deconvolution uncertainty, and experimental condition fluctuations that are almost negligible.

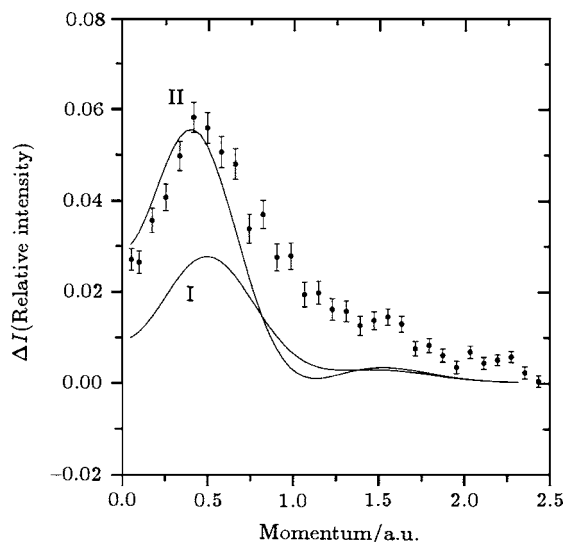


**Fig.4.** Differences of measured and calculated momentum distributions between energy regions  $11.9 \text{ eV} < E < 12.8 \text{ eV}$  and  $12.8 \text{ eV} < E < 13.7 \text{ eV}$ . The calculation is at the B3LYP/AUG-cc-pVTZ level folded with the experimental momentum resolution. See text for details.

Since the theoretical calculation fails to reproduce the experimental momentum distribution of  $3b_2+5a_1+1a_2$ , the ordering of these orbitals cannot be determined by the above mentioned method. As for the orderings  $2b_1$ ,  $4a_1$  and  $2b_2$ , Ref.[7] concluded that  $(2b_2, 4a_1) < 2b_1$ , i.e. the orbital with an ionization potential of  $20.4 \text{ eV}$  was  $2b_1$ . However, all other calculations

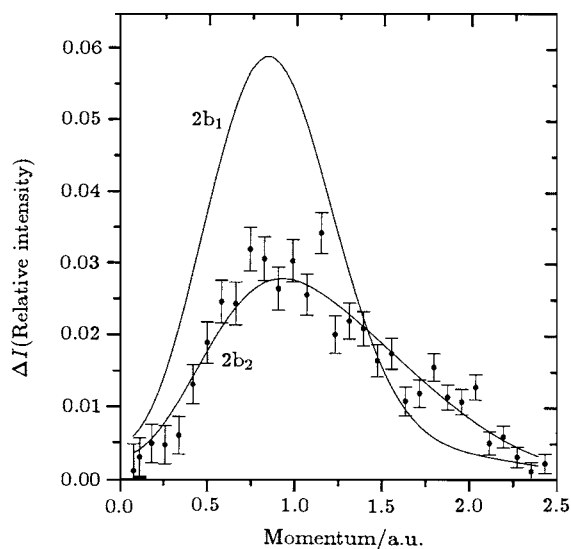


**Fig.5.** Measured spherically averaged momentum profiles for orbitals with an ionization potential of  $20.4 \text{ eV}$  of  $\text{CF}_2\text{Cl}_2$  and calculated ones with different orbital assignments. The calculation is at B3LYP/AUG-cc-pVTZ level folded with the experimental momentum resolution.

and measurements in Table 1 assign it to  $2b_2$ , and, as Fig.5 shows, our experimental momentum distribution also supports that it is  $2b_2$  orbital. Due to the small energy gap between  $2b_1$  and  $4a_1$ , it is impossible to determine their ordering by the present EMS spectrometer because a PES spectrometer with an energy resolution of  $30 \text{ meV}$  still cannot resolve them<sup>[5]</sup> and even indicate any discernable shoulder. So, it is safe to conclude that the ordering in the  $Z$ -matrix 2 coordinate system is

$$4b_1 < 2a_2 < 4b_2 < 6a_1 < 3b_1 < (5a_1, 3b_2, 1a_2) < (2b_1, 4a_1) < 2b_2 < 3a_1.$$

The orderings in parentheses need further confirmation with a more accurate experiment.

## 4. Summary

In summary, the outer valence orbitals of  $\text{CF}_2\text{Cl}_2$  have been studied using the electron momentum spectroscopy at an impact energy of  $1200 \text{ eV}$  plus binding energy. The experimental electron momentum profiles are compared with DFT and HF calculations, and the calculations well describe the experimental momentum distribution generally. The relationship between the orbital assignments in different coordinate systems is discussed. A new method of difference analysis is used to clarify the ambiguities regarding the orbital ordering. The ordering in the  $Z$ -matrix 2 coordinate system is obtained.

## Appendix

$Z$ -matrix of  $\text{CF}_2\text{Cl}_2$ .

$Z$ -matrix 1	$Z$ -matrix 2
C	C
X 1 R0	X 1 R0
F 1 R1 2 A1	CL 1 R1 2 A1
F 1 R1 2 A1 3 A2	CL 1 R1 2 A1 3 A2
CL 1 R2 2 A3 3 A4	F 1 R2 2 A3 3 A4
CL 1 R2 2 A3 3 A5	F 1 R2 2 A3 3 A5
R0 10.0	R0 10.0
R1 1.340	R1 1.780
R2 1.780	R2 1.340
A1 54.5	A1 54.5
A2 180.0	A2 180.0
A3 125.5	A3 125.5
A4 90.0	A4 90.0
A5 -90.0	A5 -90.0

## References

- [1] Irikura K K, Ali M A and Kim Y K 2003 *Int. J. Mass. Spectrom.* **222** 189
- [2] Zhang S F, Su G L *et al* 2005 *Acta Phys. Sin.* **54** 1552 (in Chinese)
- [3] Solomon S 1999 *Rev. Geophys.* **37** 275
- [4] Pradeep T and Shirley D A 1993 *J. Electron Spectrosc. Relat. Phenom.* **66** 125
- [5] Cvitaš T, Güsten H and Klasinc L 1977 *J. Chem. Phys.* **67** 2687
- [6] Cooper G, Zhang W Z and Brion C E 1990 *Chem. Phys.* **145** 117
- [7] Chen X J, Zhou L X, Zhang X H *et al* 2004 *J. Chem. Phys.* **120** 7933
- [8] Lewerenz M, Nestmann B, Bruna P J and Peyerimhoff S D 1985 *J. Mol. Struct.: THEOCHEM* **123** 329
- [9] Leung K T and Brion C E 1985 *Chem. Phys.* **95** 241
- [10] Takeshita K 1990 *J. Mol. Spectrosc.* **142** 1
- [11] Minchinton A, Cook J P D and Weigold E 1987 *Chem. Phys. Lett.* **113** 251
- [12] Deng J K, Li G Q, He Y *et al* 2001 *J. Chem. Phys.* **114** 882
- [13] McCarthy I E and Weigold E 1991 *Rep. Prog. Phys.* **54** 789
- [14] Coplan M A, Moore J H and Doering J P 1994 *Rev. Mod. Phys.* **66** 985
- [15] Weigold E and McCarthy I E 1999 *Electron Momentum Spectroscopy* (New York: Kluwer)
- [16] Wu X J, Chen X J, Shan X, Chen L Q and Xu K Z 2004 *Chin. Phys.* **13** 1857
- [17] MiGdall J N, Coplan M A, Hench D S *et al* 1981 *Chem. Phys.* **57** 141
- [18] Rolke J, Zheng Y, Brion C E *et al* 1999 *Chem. Phys.* **244** 1
- [19] Deng J K, Li G Q, Huang J D *et al* 2002 *Chin. Phys. Lett.* **19** 47
- [20] Xu C K, Chen X J, Jia C C *et al* 2002 *Chin. Phys. Lett.* **19** 1795
- [21] Su G L, Ren X G *et al* 2005 *Acta Phys. Sin.* **54** (in Chinese)
- [22] Brion C E, Zheng Y, Rolke J *et al* 1998 *J. Phys. B: At. Mol. Opt. Phys.* **L223** 31
- [23] Brion C E, Cooper G, Feng R and Tixier S 2002 *Correlations, Polarization and Ionization in Atomic System AIP CP604* 38
- [24] Ren X G, Ning C G, Deng J K *et al* 2005 *Phys. Rev. Lett.* **94** 163201